All-Regions Tunable High Harmonic Enhancement by a Periodic Static Electric Field

Carles Serrat[1,2,*] and Jens Biegert[1,3]

[1]ICFO-Institut de Ciencies Fotoniques, Mediterranean Technology Park, 08860 Castelldefels (Barcelona), Spain
[2]DTDI-Universitat de Vic, Carrer de la Laura 13, 08500 Vic (Barcelona), Spain
[3]ICREA-Institucio Catalana de Recerca i Estudis Avançats, 08010 Barcelona, Spain

(Received 26 October 2009; published 16 February 2010)

Simulations show that a static electric field periodically distributed in space can be used to control the production of coherent light by high-order harmonic generation in a wide spectral range covering extreme-ultraviolet and soft x-ray radiation. The radiation yield is selectively enhanced due to symmetry breaking induced by a static electric field on the interaction between the driving laser and the medium. The spectral position of the enhancement is tuned by varying the periodicity of the static electric field which matches twice the coherence length of the harmonics in the desired region. We find that the static electric field strength inducing enhancement decreases for shorter wavelengths and predict an increase of more than two orders of magnitude for harmonics in the water window spectral range with a static electric field as weak as 1.12 MV/cm.

DOI: 10.1103/PhysRevLett.104.073901 PACS numbers: 42.65.Ky, 32.80.Fb, 32.80.Rm

The generation of coherent light in the short wavelength region of the electromagnetic spectrum by high harmonic generation (HHG) has been extensively studied and important advances have recently been made [1–4]. Potential applications suffer from the low efficiency of HHG especially for high photon energies typically near the cutoff region. In this regard, the effect of a static electric field has received considerable attention in the last few years. Adding an electric field with a constant strength in the time scale of the nonlinear HHG process is known to cause several effects; for instance, it enhances the yield of the harmonics on the plateau [5,6], it can extend the plateau beyond the usual cutoff energy, and in some cases it produces a second plateau at higher energies [7]. Indeed the presence of a static electric field breaks the inversion symmetry in the nonlinear process of the driving laser interacting with the atom or molecule, which can result in double-plateau scenarios and produce together even and odd-order harmonics [8,9]. A static electric field has proven to be a very sensitive means for controlling the generation of high-order harmonics.

The limitation in the conversion efficiency of HHG is mainly due to the difficulty to phase match the nonlinear process, and the challenge is thus to correct for this phase mismatch at photon energies covering from the extreme-ultraviolet to the x-ray regions of the spectrum. Different approaches have been investigated to date to overcome this problem. Conventional phase matching using different driving laser wavelengths requires pressure tuning and the enhancement of HHG is obtained only at specific regions [10,11]. The increase of the conversion efficiency has also been investigated by using nonadiabatic self-phase matching techniques [12,13], where the coherence length of the nonlinear conversion is extended due to the subcycle evolution of an intense few-cycle pulse. This method is however limited to very short propagation distances due to absorption and defocusing of the driving laser and does not work close to the cutoff. Quasiphase matching techniques, on the other hand, have been used to tune a larger range in the harmonics spectrum. For example, modulated waveguides which periodically modulate the laser intensity were considered in [14–16], but in this case the energy of the enhanced harmonics is limited by the waveguide diameter which sets the minimum modulation period effective for enhancement. Other techniques use a train of counterpropagating pulses [17,18] such that the harmonic emission is suppressed in the propagation regions where the driving field is out of phase with respect to the generated harmonics, or a counterpropagating quasi-cw field, which mediates a sinusoidal modulation of the phase of the emitted harmonics [19] with a comparable result. However, although these two last methods succeed to enhance a particular region of the harmonic spectrum, the ability for tuning is limited by the physical mechanism implementing the phase-matching effect. In the first case, the separation between pulses provides the tuning mechanism, which limits the enhanced region to periods of some micrometers, and in the second case the spectral selectivity arises from the wavelength of the perturbing cw field, which confines its applicability to relatively large photon energies. Finally, phase matching by considering Bessel pulses [20] is promising in that slow intensity and carrier-envelope phase modulations can enhance photon yields in the extreme-ultraviolet spectral range by means of a sophisticated harmonics phase modulation effect, although this technique also fails to tune the multiple regions of interest.

The method that we present allows enhancement of harmonic yield near the cutoff region, it is tunable in the short wavelength range of the electromagnetic spectrum,

 © 2010 The American Physical Society

and is relatively simple to implement. We exploit the sensitivity of HHG on the driving electric field shape [21] and consequently to a symmetry breaking of the single-atom microscopic response induced by an added static electric field [8]. Our approach is based on adding such a static electric field periodically along propagation direction to the driving laser field effectively influencing the nonlinear interaction in the sense that the resulting driving field is altered in one direction along the field polarization direction. In the semiclassical picture of HHG, this will result in a slight modulation of the quantum paths that the classical electron takes in the continuum and therefore the amplitude and phase of the radiated harmonics. Affecting the microscopic response through a periodically added static field will then lead to a collective phase-matched conversion process. We carefully tailor the geometry of the interaction volume, the strength of the driving field and the length of the zones over which the static field is added such as to sum enough phase to the already accrued slippage from the driving laser for the total emission to add constructively. As we will show, for the first time the HHG enhancement can be tuned without limitations from the phase-matching mechanism, covering all characteristic coherence lengths from extreme-ultraviolet to x-ray radiation.

To demonstrate our technique in a simple case we consider a laser pulse linearly polarized in x direction with Gaussian temporal and spatial distributions of 5 fs and 40 μm diameter of focus (FWHM), central wavelength of 800 nm and peak intensity at focus 7×10^{14} W/cm^2. This pulse propagates from the focus into a gas medium producing high harmonics with a photon energy cutoff at $\approx$ 154.16 eV. The medium that has been chosen in our calculations is neon (ionization potential 21.56 eV) at 20 mbar. As illustrated in Fig. 1(a), our phase-matching scheme is based on the presence of a static electric field spatially distributed in the direction of propagation and oriented in the same direction as the polarization of the laser field, i.e., the x direction in this case. We performed numerical simulations based on a three-dimensional propagation model in cylindrical coordinates using the nonadiabatic strong-field approximation [22] to calculate the atomic response, as outlined in [23]. The input laser field can be written as $E = E_0 \exp[-(r/\rho)^2] \exp[-(t/\tau)^2] \times \cos(\omega_L t + \phi)$, where E_0 is the peak amplitude at focus, r and t are the radial and temporal variables, ρ and τ provide the width of the transverse and temporal profiles, respectively, ω_L is the central angular frequency of the laser and ϕ the initial phase. The static electric field is taken into account by adding a constant value $\xi\beta E_0$ to the laser field, distributed such that $\xi = 0$ at $2n\Delta_s < z < (2n+1)\Delta_s$ and $\xi = 1$ elsewhere, with z being the longitudinal coordinate and $n = 0, 1, 2, \ldots$. The strength of the static electric field is thus defined by the parameter β, which is the fraction of the laser peak amplitude at focus, and Δ_s is half the period of the static electric field distribution.

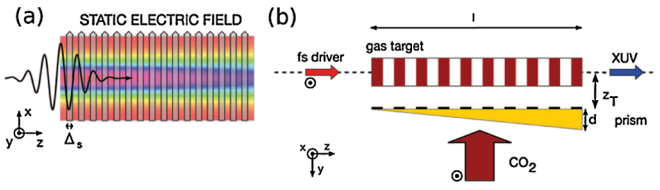

FIG. 1 (color online). (a) Focused laser pulse linearly polarized in x direction propagating in a medium with a periodically distributed static electric field also oriented in the x direction. (b) Implementation of the periodic electric field: A pulsed CO_2 laser is collimated and sent through a small wedge with a binary amplitude mask whose amplitude pattern generates the desired periodic field modulation after each multiple of the Talbot distance z_T. The wedge ensures equal field strengths of the periodic pattern.

In the results displayed in Fig. 2 the peak amplitude of the driving laser field at focus is taken as $E_0 \approx$ 726 MV/cm, and we have considered a static electric field such that $\beta = 0.01$ with different periodicities, as indicated. As it is clear from the simulations, the spectral region that corresponds to harmonics H93–H99 near the cutoff ($\approx$140–160 eV) can be enhanced with respect to the spectrum obtained in the absence of the static electric field (black line) by more than two orders of magnitude, which has been computed in this case with a static electric field periodicity such that $\Delta_s = 125$ μm (red line). Figure 2 also shows how increasing the period of the static electric field spatial distribution in the enhanced region shifts to lower photon energies in the spectrum. Furthermore, the cutoff is not extended for the static electric field values used in our simulations when a periodicity shorter than the coherence length of the cutoff harmonics is chosen (see the gray line in Fig. 2 for $\Delta_s = 100$ μm). Indeed, the coher-

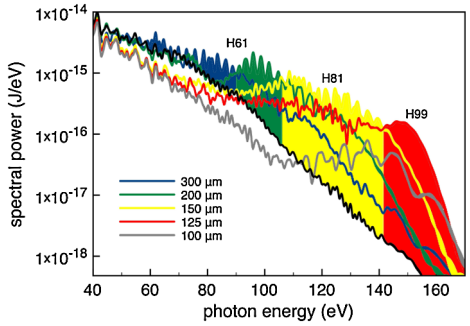

FIG. 2 (color online). Spectral power of the harmonics (radially integrated spectral energy—in Joules per photon energy unit—in eV) versus photon energy near the cutoff region after a propagation distance of 2 mm with $E_0 \approx$ 726 MV/cm and $\phi = 0$. The black line corresponds to $\beta = 0$, and the other lines show the calculations for a static electric field strength such as $\approx$7.26 MV/cm ($\beta = 0.01$) spatially distributed along the z direction, with periodicities $\Delta_s = 100$ μm, 125 μm, 150 μm, 200 μm, and 300 μm as indicated. The colored areas indicate the photon yield enhancement with respect to $\beta = 0$ with a maximum efficiency tuned by Δ_s.

ence length of the different harmonics, which is usually defined as $L_{c_q} = \pi/|\Delta k_q|$, with $\Delta k_q = qk_l - k_q$ being the difference between q times the laser and the q-order harmonic wave vectors, can be computed numerically from the evolution in z of each harmonic in the absence of static electric field ($\beta = 0$).

The static electric field periodicity needed to enhance the region near the cutoff corresponds to the coherence length of the harmonics H93–H99. The coherence length depends on the interaction parameters, and decreases as a function of the harmonic order as $1/(n_e q)$, where n_e is the plasma electron density [18]. The enhanced harmonics region can thus be tuned using our phase-matching technique by simply increasing or decreasing the period of the static electric field distribution. Figure 3(a) shows the growth of different harmonics along propagation for $\beta = 0.01$ together with the corresponding behavior without the influence of the static electric field [Fig. 3(b)]. The steplike increase observed for $\beta = 0.01$ is typical for quasiphase matching mechanisms. In Fig. 3(b), a slight change of the coherence length (L_{c_q}) of the different harmonics as a function of the propagation distance can be appreciated, which is expected due to different propagation effects such as group-velocity dispersion and refraction [18]. This last effect can be fine adjusted by matching the evolving coherence length with the period of the static electric field distribution along z. The static electric field and spatial distributions used in our simulations can be implemented in the experiment in a very simple and elegant way with an optical interferometry technique and a long-wavelength laser. Figure 1(b) shows such implementation with only one optical element; it should therefore be simple to realize experimentally. We propose to use a binary amplitude mask on the transverse profile of a CO_2 laser making an array illuminator based on the Talbot effect [24]. The mask is deposited onto a small prism which is used for synchronizing the CO_2 pulses with the driving field along the interaction region, which is placed at the Talbot distance $z_T = 2a^2/\lambda_{CO_2}$, where $a = 2\Delta_s$. The electric field strength and periodicities required to reproduce experimentally the simulations reported in Fig. 2 can readily be obtained with this scheme considering state of the art CO_2 laser technology, using, e.g., a ZnSe prism of thickness $d = 833$ μm and a 10.6 μm CO_2 laser of 1 J/pulse and 0.5 ns pulse duration.

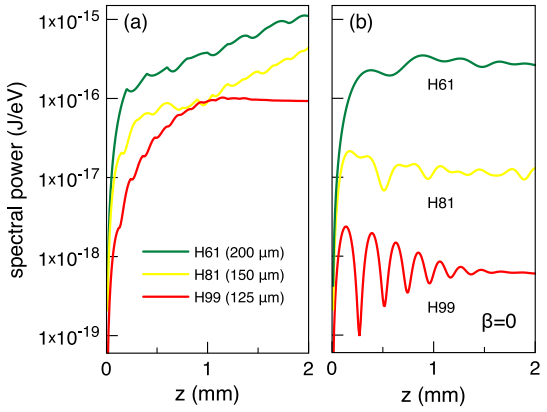

FIG. 3 (color online). Evolution of the spectral power for different harmonics as a function of the propagation distance z with $\beta = 0.01$ (a). The dynamics with no static electric field ($\beta = 0$) is shown in (b), from where the coherence length L_{c_q} is evaluated.

To demonstrate tunability of our method towards higher spectral energies, we carried out calculations with doubly ionized Ne ions (ionization potential 63.45 eV) as the interacting medium, increased the peak intensity of our beam up to 3×10^{15} W/cm^2, used $\Delta_s = 32$ μm, and kept the other parameters as in the previous simulations. This new configuration gives a cutoff of the generated harmonics at 631.75 eV, well into the soft x-ray water window spectral range. We find that as the energy of the generated harmonics increases, the strength of the static electric field that is needed to enhance the harmonics yield decreases substantially, which is consistent with the results reported in [19]. In Fig. 4 we illustrate the results obtained for the enhancement in these higher photon energies. Spectra for $\beta = 0$ and for a strength of the periodic static electric field such that $\beta = 7.5 \times 10^{-4}$ at a propagation of 0.3 mm are

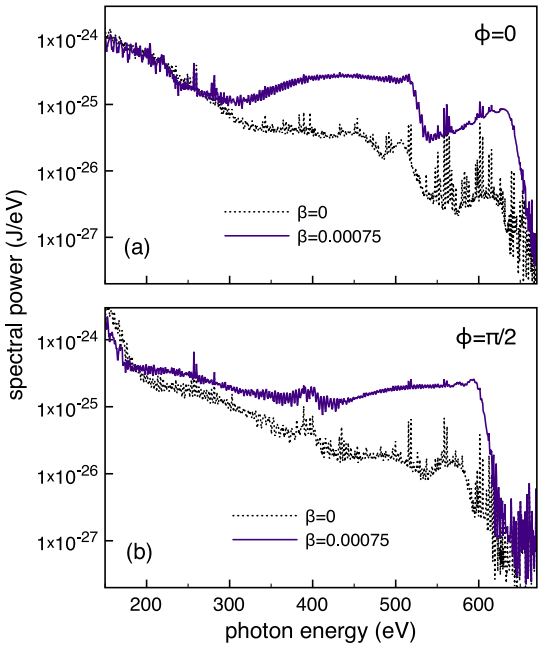

FIG. 4 (color online). Spectral power of the harmonics (radially integrated spectral energy—in Joules per photon energy unit—in eV) versus photon energy near the cutoff region after a propagation distance of 0.3 mm with a static electric field periodicity such that $\Delta_s = 32$ μm. In (a) the carrier-envelope phase of the driving field is $\phi = 0$; the dotted black line corresponds to $\beta = 0$ (absence of static electric field), and the violet full line shows the calculations with $\beta = 7.5 \times 10^{-4}$ (1.12 MV/cm). In (b) the carrier-envelope phase of the driving field is $\phi = \pi/2$, and the other parameters are as in (a), as indicated.

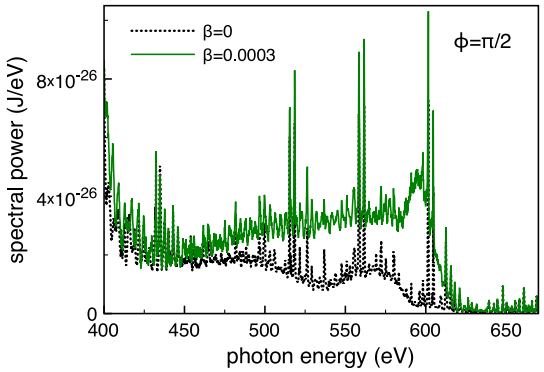

FIG. 5 (color online). The spectral power obtained with $\beta = 3 \times 10^{-4}$ (450 kV/cm) is compared to the case with no electric filed ($\beta = 0$). The initial phase is $\phi = \pi/2$ and the other parameters are as in Fig. 4. The enhanced region results highly localized at about 580–600 eV.

shown. The effect of the carrier-envelope phase ϕ on the generated harmonics for an intense ultrashort driving pulse such as the one we are considering is known to be important with reported phase-dependent effects near the high-harmonics cutoff [25]. It is thus worth considering whether the enhancement mediated by our periodic static electric field is also sensitive to the carrier-envelope phase. With this purpose, we have calculated the generated spectra for two different values of the initial carrier-envelope phase, $\phi = 0$ and $\phi = \pi/2$. As it is shown in Figs. 4(a) and 4(b), the localization of the enhancement is well centered in the cutoff region of the spectra, as expected for $\Delta_s = 32$ μm. Moreover, we find that the regions of maximum enhancement efficiency are clearly correlated to the carrier-envelope phase-dependent spectra in the absence of the static electric field ($\beta = 0$). This phase effect can certainly be used as a carrier-envelope phase measurer. It is also worth noting that the spectral width of the enhanced yield, which is about 150–200 harmonic orders ($\approx$300 eV) in our simulations, can be associated to the small variation of the coherence length of the corresponding harmonics in this region, and agrees well with what was previously reported by using other enhancement mechanisms [19]. Indeed, at this gas pressure (20 mbar), the coherence length for H407 (631.75 eV) is roughly 32–38 μm and for H257 (398.29 eV) is 35–42 μm. Our simulations therefore predict an enhanced coherent radiation of more than two orders of magnitude in the soft x-ray spectral range, which is mediated by a static electric fields as weak as 1.12 MV/cm. Finally, if we reduce the strength of the static electric field in these operating conditions the enhancement can be localized in a narrow spectral range of a few tenths of eV, as it is shown in Fig. 5 where a sharp localization in the range 580–600 eV has been obtained with $\beta = 3 \times 10^{-4}$ (450 kV/cm).

In summary, we have reported a novel phase-matching effect for high-order harmonic generation to enhance the yield of the coherent radiation near the cutoff region by more than two orders of magnitude; tunability of the enhancement in all regions of the spectrum can be accomplished by varying the strength and periodicity of a spatially distributed static electric field covering the interaction region. The effect of the initial phase ϕ on the enhanced harmonics provides a precise carrier-envelope measurer which will be described elsewhere. The periodicities and strengths of the static electric field needed to implement our scheme are relatively high for low photon energies but they decrease for higher photon energies being attainable in practice by optical interferometry techniques. In previous research different mechanisms have been extensively investigated which are capable to enhance the harmonic yields, in particular, spectral ranges and interacting conditions. For the first time a method that is able to tune the HHG enhancement to cover all characteristic coherence lengths from extreme-ultraviolet to x-ray radiation without limitations from the phase-matching mechanism is reported. This work thus represents an important advance in overcoming a critical challenge in high-order harmonic generation and coherent x-ray science.

We would like to thank Dr. D. Zalvidea for helpful discussions. Support is acknowledged from the Spanish Ministry of Education and Science through its Consolider Program Science (SAUUL-CSD 2007-00013), through "Plan Nacional" (FIS2008-06368-C02-01/02), as well as from the Barcelona Supercomputing Center.

*carles.serrat@icfo.es

[1] T. Popmintchev *et al.*, Proc. Natl. Acad. Sci. U.S.A. **106**, 10 516 (2009).
[2] A. Paul *et al.*, IEEE J. Quantum Electron. **42**, 14 (2006).
[3] H. C. Kapteyn *et al.*, Phys. Today **58**, No. 3, 39 (2005).
[4] T. Brabec *et al.*, Rev. Mod. Phys. **72**, 545 (2000).
[5] M.-Q. Bao and A. F. Starace, Phys. Rev. A **53**, R3723 (1996).
[6] B. Borca *et al.*, Phys. Rev. Lett. **85**, 732 (2000).
[7] A. Lohr *et al.*, Laser Phys. **7**, 615 (1997).
[8] B. Wang *et al.*, J. Phys. B **31**, 1961 (1998).
[9] W. Hong *et al.*, J. Phys. B **40**, 2321 (2007).
[10] T. Pfeifer *et al.*, Rep. Prog. Phys. **69**, 443 (2006).
[11] T. Popmintchev *et al.*, Proc. Natl. Acad. Sci. U.S.A. **106**, 10516 (2009).
[12] G. Tempea *et al.*, Phys. Rev. Lett. **84**, 4329 (2000).
[13] M. Geissler, G. Tempea, and T. Brabec, Phys. Rev. A **62**, 033817 (2000).
[14] I. P. Christov *et al.*, Opt. Express **7**, 362 (2000).
[15] A. Paul *et al.*, Nature (London) **421**, 51 (2003).
[16] E. A. Gibson *et al.*, Science **302**, 95 (2003).
[17] J. Peatross *et al.*, Opt. Express **1**, 114 (1997).
[18] X. Zhang *et al.*, Nature Phys. **3**, 270 (2007).
[19] O. Cohen *et al.*, Phys. Rev. Lett. **99**, 053902 (2007).
[20] D. Faccio *et al.*, Phys. Rev. A **81**, 011803(R) (2010).
[21] J. Peatross *et al.*, J. Opt. Soc. Am. B **12**, 863 (1995).
[22] M. Lewenstein *et al.*, Phys. Rev. A **49**, 2117 (1994).
[23] E. Priori *et al.*, Phys. Rev. A **61**, 063801 (2000).
[24] W. H. F. Talbot, Philos. Mag. **9**, 401 (1836).
[25] A. Baltuska *et al.*, Nature (London) **421**, 611 (2003).